Astron. Astrophys. 335, 881–893 (1998)

ASTRONOMY AND ASTROPHYSICS

Optically thin thermal emission from cold clouds in active galactic nuclei

G. Torricelli-Ciamponi[1,2] **and T.J.-L. Courvoisier**[1,3]

[1] Geneva Observatory, ch. des Maillettes 51, CH-1290 Sauverny, Switzerland
[2] Osservatorio di Arcetri, Largo E.Fermi 5, I-50125 Firenze, Italy
[3] ISDC, ch. d'Ecogia 16, CH-1290 Versoix, Switzerland

Received 30 September 1997 / Accepted 6 April 1998

Abstract. The thin thermal emission from an ensemble of cold condensations embedded in a hot plasma is investigated. The temperature distribution inside the cloud is derived by integrating the energy equation where heating, radiative losses and thermal conduction balance each other. The presence of the thermal conduction term, which constitutes the main difference with respect to the previous models, determines the scale length of the cloud and makes the cold cloud core very narrow while the surrounding shell, only slightly cooler than the external medium, is very extended. It follows that the emission from the cold core is negligible with respect to that of the extended shell, which in turn can be more luminous than the surrounding medium only if a strong negative pressure gradient is introduced. Hence, the emission from such a configuration does not show a thermal peak characterized by a temperature value ranging from 10^5 to $10^6 K$ as observed in the active galactic nuclei (AGN) spectra. These conclusions are independent of the selected heating and loss functions and also the introduction of a magnetic field cannot change them. If evolving structures can be a viable solution to this problem is also briefly analyzed.

Key words: radiation mechanisms: thermal – ultraviolet: galaxies – galaxies: nuclei – galaxies: Seyfert – galaxies: quasars: general

1. Introduction

It is commonly accepted that active galactic nuclei (AGN) emission is powered by accretion onto a central black hole. How this accretion takes places is still a matter of debate even if a disk-like geometry seems preferred with respect to a spherical accretion (Collin-Souffrin 1991). In both cases accreting matter can be responsible at least for part of the thermal radiation excess present in quasar and Seyfert 1 spectra, the so called big blue bump. This thermal component extends from energies of about 1 eV up to 100 eV, possibly including also the soft-X ray excess, and peaks in the ultraviolet (UV) domain. Shields (1978) was the first to propose the disk as the origin of the blue bump. Disks are able to account for many observed AGN properties but, in their simplest versions, have difficulties in explaining the observed variability in the UV and optical continuum (Clavel et al. 1991) and the far UV and soft X-ray part of the spectrum (see Courvoisier & Clavel 1991 for a review on this topic). For these reasons more complex disk models have been developed in the last years (see for example Ross et al. 1992 and, for disks with a hot corona, Haardt et al. 1994, Życki et al. 1995) and, on the other hand, the possibility of explaining the observed optical-UV spectrum via cold cloud emission has been proposed by Barvainis (1993).

Many authors have computed the out-coming radiation from an assembly of cold optically thick clouds (Lightman & White 1988, Sivron & Tsuruta 1993) or, more recently, cold optically thin clouds (Barvainis 1993, Collin-Souffrin et al. 1996). Detailed comparison with observations have shown that optically thin clouds, at least in their simplest single temperature form, have also problems in reproducing all the emission properties (Siemiginowska et al. 1995, Fiore et al. 1995). A more complex modelization is then needed.

Still in the framework of thin clouds, but in a different range of density, the structure of much more dense, optically thin filaments has been investigated by Celotti et al. (1992). The emission of such condensations has been proved to be not suitable for reproducing the observed spectrum (Kuncic et al., 1997).

Given the high number of free parameters, the hypothesis of thermal emitting clouds is difficult to exclude on the basis of the emission features only. For this reason, in this paper we address the problem from a different point of view investigating whether clouds of properties such that they could contribute to the blue bump can really exist in AGNs. We neglect for the moment the cloud motion in the neighborhood of the AGN nucleus and the role they play in the accretion. Clouds can be a working model for explaining the thermal part of the AGN spectrum only if in the vicinity of a AGN nucleus such condensations can: i) form, ii) be alive for a sufficient long time and iii) have thermodynamic parameters with which the bulk of the observed UV radiation can be reproduced. These three conditions are equally necessary for modeling the UV spectrum. If only one of them fails clouds cannot be a possible explanation for UV radiation and the search for a detailed matching between the theoretically derived emission and the observed radiation is pointless. For this reason we

Send offprint requests to: G. Torricelli (Arcetri)

will focus our attention in investigating if stable condensations satisfying the most important observed properties of AGN can exist.

Among the several features that characterize AGN emission we have chosen those which are common to most of the objects and which are essential for the construction of an appropriate model. They are the following:

1) Optical-UV emission is variable on time-scales as short as a week thus implying a radiating structure of an extension $R_{UV} \lesssim 10^{16} cm$ and hence not more distant from the nucleus than R_{UV} itself.

2) The emission shows a thermal spectrum characterized by a temperature $T \simeq 10^5 K$ which can be as high as 10^6 if the soft X-ray excess is included, as Walter & Fink (1993) results suggest. In the neighborhood of the AGN nucleus the plasma is easily much hotter than this (as one can infer from equipartition) and hence optical-UV radiation comes from cold condensed matter.

3) The spectral steepening observed by OSSE around 100 keV (see Zdziarski et at. 1995 and references therein) implies that the condition $L_X > L_{UV}$ does not always hold. Hence, UV radiation cannot be generally assumed to be a byproduct of X-ray radiation even if some interaction between the two energy bands exists, as shown by the reprocessing features in the X-ray energy band and implied by the theory of Compton and inverse-Compton processes.

One possible working hypothesis, followed in this paper, is that the UV emission is not entirely radiatively fueled by X-ray radiation but that some independent mechanical heating contributes to the energy supply of the blue bump. Therefore, to make the treatment as general as possible, the existence of both radiative and mechanical heating is taken into account and various forms for radiative losses are considered.

The paper is organized as follows: in Sect. 2 the role of thermal conduction is introduced; in Sect. 3 the assumed representative loss and heating functions are illustrated. The temperature and luminosity profiles inside the cloud are derived in Sects. 4 and 5, respectively. In the next sections the influence of different initial hypothesis is analyzed by deriving the corresponding temperature profile when pressure gradients (Sect. 6) and an external magnetic (Sect. 7) are introduced and by testing the assumption of a stationary configuration (Sect. 8). The possibility of an evolving equilibrium is investigated in Sect. 9.

2. Looking for equilibrium configurations

2.1. The equations

Suppose that condensations can form from the hot medium surrounding AGN cores and that these condensations can attain their final configuration on the correct time scale (which is not obvious as Mathews & Doane (1990) have shown for Broad Line Region clouds). Suppose also that these blobs are then entrained in the flow of the medium from which they originated, since any relative displacement will facilitate their disruption owing to hydrodynamic instabilities. We are now confronted to test the validity of point iii) of the introduction.

A stationary configuration of cool clouds embedded in a hot plasma must satisfy the stationary momentum

$$\rho \mathbf{v} \cdot \nabla \mathbf{v} = -\nabla p + \mathbf{J} \times \mathbf{B} - \rho \mathbf{g} + \mathbf{F_{ext}}. \qquad (1)$$

and energy

$$\frac{\rho^\gamma}{\gamma - 1} v \cdot \nabla (p\, \rho^{-\gamma}) = 0 = L - H - \nabla \cdot (\kappa \nabla T) \qquad (2)$$

equations. Here ρ, T, $\mathbf{v}$ and p are the plasma density, temperature, velocity and pressure, γ is the ratio of the plasma specific heat at constant pressure to that at constant volume, $\mathbf{g}$ is the cloud self gravitational acceleration, $\mathbf{J} = \nabla \times \mathbf{B}/4\pi$ with $\mathbf{B}$ the magnetic field and $\mathbf{F_{ext}}$ are other eventually present external forces. On the right-hand side of Eq. (2) the first term represents radiative losses, the second is the heating rate and the third is the thermal conduction ($\kappa = \kappa_o T^{5/2} \simeq 10^{-6} T^{5/2}$ $erg/(cm\ sec\ K)$ (Spitzer, 1962)). The specific form of heating and loss functions depend on the problem under study and on the the related hypotheses, as explained hereafter.

2.2. Disregarding thermal conduction

Usually, when two phase equilibria are investigated the pressure is assumed as constant supposing that the cloud and the external confining medium have the same pressure and conduction is disregarded in the static and stationary energy equation (see for example Krolik et al. (1981) for Broad Line Regions and Reynolds & Fabian (1995) for the case of the warm absorber). In terms of temperature distribution this last point implies that a stepwise temperature profile is assumed, while, in reality, conduction will smooth it, transporting heat from the hot inter-cloud medium to the cold cloud core. The idea is that the development of this thin region of intermediate temperature will not substantially change the results obtained disregarding the conduction term. We follow this approach here and will consider the effects of conduction in Sect. 2.3.

Solving the energy equation in the above limits (static and stationary equations with constant pressure and no conduction) means equating loss and heating terms $L(p,T) = H(p,T)$ and deriving from it the possible equilibria $p(T)$. Each heating curve can have one or more intersections with the radiative loss curve, hence different equilibria at different temperatures but with the same pressure are possible. However, not all of them are acceptable since only temperature intervals for which $\frac{\partial[(L-H)/n]}{\partial T}|_{p=const.} > 0$ can correspond to stable equilibria (Field 1965). Hence even in this simplest version the possibility of a two phase configuration is not straightforward and demands the existence of specific $(L-H)$ functions. In general, the assumption of *coronal* radiative losses, having a peak around $T \simeq 10^5 K$, assures that the first intersection at low temperatures is stable.

This procedure allows us to derive two different temperature values (that of the cloud and that of the confining medium) for a given pressure but determines neither the pressure value nor the cloud dimension. More than that, since the real nature of

the heating term is not known and heating parameters can also be freely changed, cloud and confining medium parameters remain almost completely undetermined and can be determined only on the basis of observational constraints. When different authors (Barvainis (1993), Collin-Souffrin et al. (1996), for example) compute the cloud emission having in mind the existence of such a two phase stepwise equilibrium they have no limits in the choice of the parameter values. Actually, in the above procedure momentum and energy equations do not play an important role in constraining the parameter range only because the simplifying hypotheses $\frac{\partial}{\partial t} = 0$, The problem lies in the specific influence that each above simplifying assumption has on the final solution. In the following sections the consequences of relaxing the above hypotheses will be analyzed.

2.3. The role of thermal conduction

If thermal conduction is not disregarded, but still in the hypothesis of a stationary, static and constant pressure plasma, the energy equation in spherical geometry becomes:

$$\kappa_o \frac{\partial}{\partial r}[r^2 T^{5/2} \frac{\partial T}{\partial r}] = r^2 [L(p,T) - H(p,T)]. \qquad (3)$$

The temperature profile is given by the solution of this equation with the boundary conditions at the cold cloud center, $r = 0$:

$$T = T_o \qquad \frac{\partial T}{\partial r} = 0.$$

The cloud extension R and the temperature of its external layer T_M are results of the integration since the boundary between the cloud and the confining medium has been defined as the place where, along the integration path, $\frac{\partial T}{\partial r} = 0$. This fact implies that neither T_M nor R can be arbitrarily chosen, their values depend on the constant parameters present in the energy equation. Normalizing heating and losses by the quantity $l_o = n_o^2 10^{-22}\ erg\ cm^{-3} sec^{-1}$ (where n_o is the cloud central number density) and taking

$$T = T_o \theta \qquad r = Z\, x \qquad (4)$$

with $0 \leq x \leq x_M = R/Z$, it follows from Eq. (3) that

$$Z = \left[\frac{T_o^{7/2} \kappa_o}{l_o}\right]^{1/2} = 10^5 \left[\frac{T_{o,4}^{7/2}}{n_{o,10}^2}\right]^{1/2} \quad cm \qquad (5)$$

where $T_{o,4}$ is the temperature expressed in units of $10^4\ K$ and $n_{o,10}$ is the number density in units of $10^{10}\ cm^{-3}$. The cloud scale lengths are, therefore, not free but, through Z, depend on the central density n_o and temperature T_o: the denser and the colder the cloud the smaller its scale length.

The temperature profiles resulting from the integration of Eq. (3) will be presented in Sect. 4. However, from this first analysis of the energy equation already comes out that the introduction of thermal conduction completely modifies the picture obtained without conduction: the cloud extension is now constrained.

3. Loss and heating functions

Defining heating and loss functions in the AGN environments is not obvious since the plasma physical conditions are not known. For this reason we tried to be as general as possible in the choice of these functions.

As far as the heating term is concerned two different contributions have been explicitly taken into account: an unknown mechanical heating and the Compton effect. The radiation heating due to photoionization from the external radiation has been included in the radiation losses, as explained in the following.

To find out which mechanical heating mechanism is efficient in such an environment is difficult. Shocks, wave dissipation, Joule heating and Coulomb collisions could be good candidates for dissipating kinetic and magnetic energy. The problem lies in their possibilities of heating an appropriate gas amount to the temperatures derived from the observed UV spectra. Some possible mechanical heatings are listed in Krolik et al. (1981) and in Gonçalves et al. (1993, 1996) for Broad Line Regions and in Rosner et al. (1978) for solar corona. All of them can be cast in a generic form

$$H_{mec} = h\, p^m T^{-s}$$

where the values of h, m and s depend on which heating mechanism is selected. For example, if energetic charged particles heat the plasma by collisions it is $H_{mec} \propto p\, T^{-1}$ (Krolik et al. 1981), while the viscous damping of acoustic modes implies $H_{mec} \propto T^2$ (Rosner et al. 1978). Clearly each heating mechanism can work only in a certain range of temperatures and different contributions for different temperature values are possible. In our analysis we assume that one or several appropriate heating mechanisms are efficient and we will change the three parameters over a certain range in order to have an idea of their influence on the final results.

The Compton contribution, related to the interaction between external X-ray photons and thermal electrons, yields an energy gain for the plasma with $T < T_C$, where T_C is the Compton temperature, and acts as a loss mechanism for the plasma having a temperature $T > T_C$. This context is different from those where the origin of UV photons is completely ascribed to the degradation of X-ray radiation since here it is not necessary to have $L_X > L_{UV}$ and Compton heating can be small in comparison with other heating processes. Following the Krolik et al.(1981) notation one obtains

$$Compton\ Contrib. = H_{Compt.} - L_{Compt.} =$$

$$= 10^{-7}\, p^2 (\frac{T_C}{T} - 1)\, \frac{F}{F_{ion}}\, \Xi \quad erg\, cm^{-3} sec^{-1} \qquad (6)$$

where

$$\Xi = 2.3 \frac{ionizing\ radiation\ pressure}{plasma\ pressure}$$

and T_C and F/F_{ion} depend on the detailed spectrum of the incident radiation. Here we have assumed $T_C = 10^8 K$ and $F/F_{ion} = 5$ (as in Krolik et al.(1981)) but we have also changed these values and we have tested that the final results do not

depend on this choice. Adding Compton losses to the other losses described hereafter, for the heating term we can generically write

$$H(p,T) = H_{mec} + H_{Compt.}.\ erg\ cm^{-3} sec^{-1} \qquad (7)$$

The best known explicit form for radiative losses in a thin plasma is the so called *coronal model*. In this approximation the plasma is not radiatively heated, but its ionization state is controlled by the balance of collisions and radiative recombinations. Radiative losses from such a thin plasma (free-free+2 photons+bound-free+bound-bound) have been computed by many authors (among them Raymond & Smith 1977, Gehrels & Williams 1993) and can be approximated in the form

$$L_{coronal} = n^2 Q_i(T) T^{\alpha_i} \ \ erg\ cm^{-3} sec^{-1}$$

where n is the number density and the function $Q_i(T)T^{\alpha_i}$ is shown in Fig. 1.

The validity of *coronal* radiative losses is limited by two different circumstances: photo-ionization by external radiation and collisional de-population of excited levels.

In the central part of the AGN the presence of external photo-ionizing radiation will be important. Therefore, in addition to the above considered case in which the contribution of external radiation in heating the plasma is negligible, it is important to weigh the influence of an ionizing external radiation on the plasma energy balance. The computation of a detailed ionization balance necessary to derive the correct loss function, in a situation which is not a pure coronal one, is out of the scope of this paper. However, it seems important to test the sensitivity of our picture to a change of the radiative loss function. To do that we have used the radiative loss function modified by the presence of photo-ionization computed by Krolik et al. (1981) (the only ones who show an explicit picture of this modified loss function). Following Krolik et al.(1981) definition, this net cooling rate Λ_{net} also includes photo-ionization heating and Compton cooling (i.e. the term $L_{Compt.}$ appearing in Eq. (6)). An approximative sketch of Λ_{net} is shown in Fig. 2 for the case of ionization parameter $\Xi = 1$. This new loss function

$$L_{Krolik.} = n^2 \Lambda_{net} \qquad (8)$$

is less efficient than the pure coronal one at low temperatures, but is more efficient at high temperatures owing to the Compton contribution.

For high density values the coronal approximation fails since collisional de-population of excited levels is not negligible anymore when compared to radiative de-population, thus requiring a different ionization balance for the plasma (see, for example, Mewe 1990). The upper limit $n \leq 7.6\ 10^5 T^2 cm^{-3}$ (Wilson, 1962) is very stringent for the cold cloud phase. For higher density values a different loss function should be assumed. However, Kuncic et al.(1997) who numerically performed the exact computation for the case of very dense plasmas conclude that line emission cooling is still partially efficient at high densities. In conclusion, both photo-ionization, which acts as an additional heating, and the collisional de-population, which reduces the emission, can be considered as having the same global effect of lowering radiative losses at low temperatures.

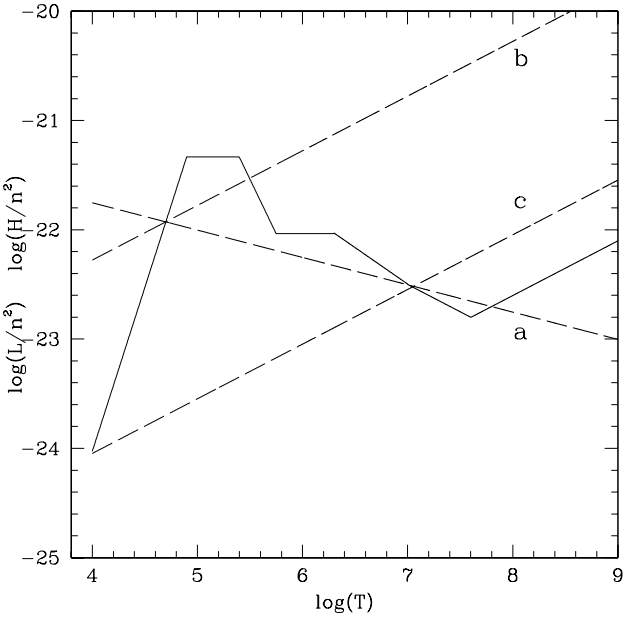

Fig. 1. *Case 1*: radiative coronal losses $L_{coronal}/n^2$ (continuous line) and three examples of heating functions H/n^2 (dashed line) as explained in the text

To understand the influence of heating and loss terms on the temperature profile and in order to make the analysis as general as possible different combinations of the heating and loss function have been investigated. Five cases have been selected as representative and are shown hereafter.

Case 1: the influence of external radiation is assumed negligible

In this case it is $\Xi < 0.1$ and

$$L(p,T) = L_{coronal} \qquad H(p,T) = H_{mec.}$$

Among a variety of possible heating functions the three reported in Fig. 1 have been chosen for their representativity. Each of the heating function has one different property in common with each of the two others thus giving the possibility of investigating which element is important: curves a and c have the same dependence on the temperature; curves a and b intersect the loss curve at the same low value of the temperature and the same holds for curves a and c at high temperature. Expressing the constant h/n_o^2 in units of $erg\ cm^3 sec^{-1}$, the heating parameters are:

Case 1a: $s = 2.25$, $m = 1$, $p_o h/n_o^2 = 4.4\ 10^{-12}$;
Case 1b: $s = 1.50$, $m = 1$, $p_o h/n_o^2 = 1.3\ 10^{-15}$.
Case 1c: $s = 1.50$, $m = 1$, $p_o h/n_o^2 = 2.2\ 10^{-17}$.

Case 2: the influence of external radiation is important

In this case both heating and losses depend on the intensity of the external radiation through the parameter Ξ ($\Xi > 0.1$) as explained before

$$L(p,T) = L_{Krolik} \qquad H(p,T) = H_{mec.} + H_{Compt.}$$

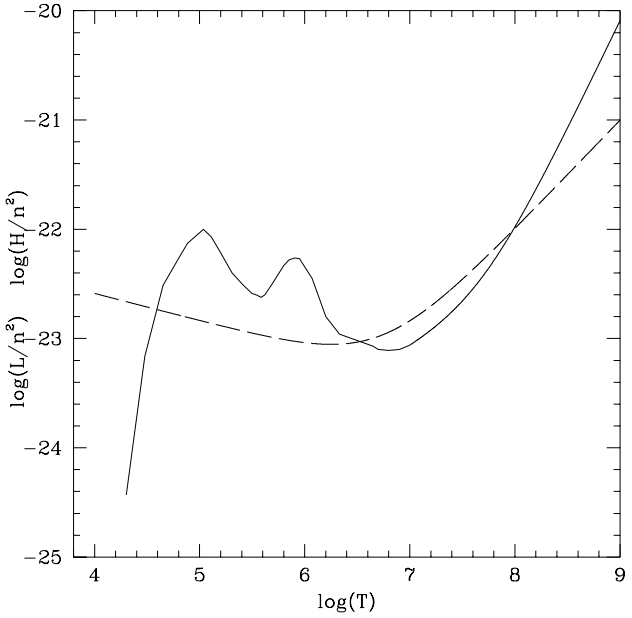

Fig. 2. *Case 2a*: radiative losses L_{Krolik}/n^2 (continuous line) and heating function, H/n^2, (dashed line) when photoionization is present and $\Xi = 1$. Radiative losses have been derived from Fig. 2 of Krolik et al.(1981)

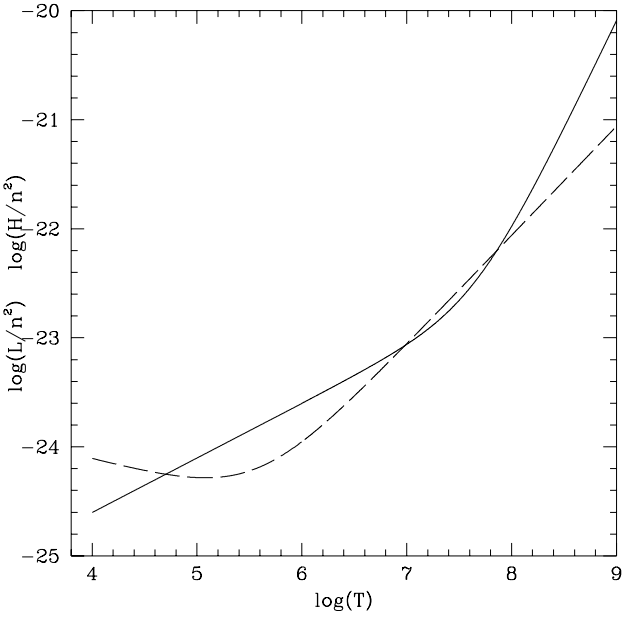

Fig. 3. *Case 3a*: radiative losses L_{ff}/n^2 (continuous line) and heating functions H/n^2 (dashed line) for $\Xi = 1$.

Case 3: extreme case in which the plasma loss function is pure free-free emission

This case seems a reasonable lower limit for every type of loss function in a thin plasma. Since also in this case external radiation is taken into account Compton gains and losses (Eq. (6)) are included. We then have

$$L(p,T) = L_{ff} + L_{Compt.} \qquad H(p,T) = H_{mec.} + H_{Compt.}$$

where

$$L_{ff} = 2.\,10^{-27}\; n^2 T^{0.5}\;\; erg\; cm^{-3} sec^{-1}.$$

For these last two cases the mechanical heating has been assumed as in *Case 1a* and different values of Ξ have been tested ranging from $\Xi = 0.1$ up to $\Xi = 10$. Figs. 2 and 3 show loss and heating functions in these two cases.

4. The temperature profile

Eq. (3) has been integrated starting from the central temperature T_o up to the temperature T_M for which the condition $\frac{\partial T}{\partial r} = 0$ is attained. The possibility of a different external boundary condition is illustrated in Appendix A. All present parameters have been changed in turn. The results presented here refer to the five cases of heating and loss functions illustrated above and to the central temperature $T_o = 5\,10^4 K$. Temperature and luminosity profiles are shown as functions of $x = r/Z$ (see Eq. (4)) where in this specific case the radius scale length, derived from Eq. (5), is

$$Z = \frac{1.7\,10^6}{n_{o,10}} \;\; cm.$$

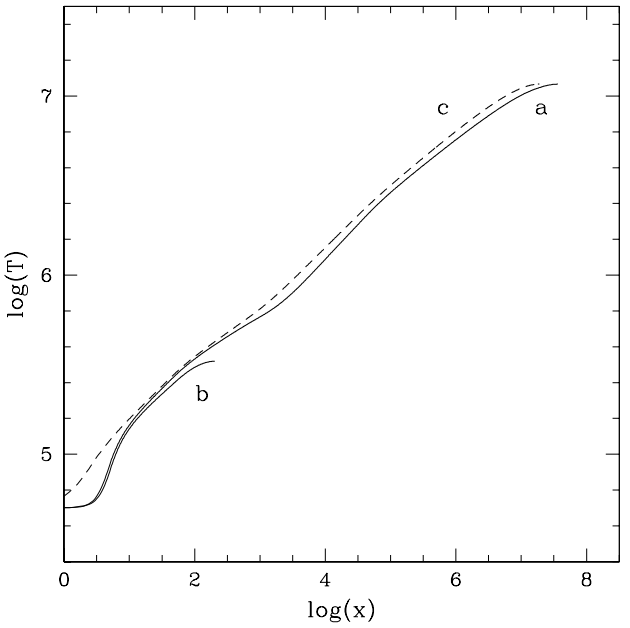

Fig. 4. Cloud temperature profile for coronal radiative losses and for the three cases of heating functions : *Cases* $1a$, $1b$ and $1c$ (see the text)

4.1. The influence of different heating functions

For *Cases 1a, 1b* and *1c* the temperature profiles resulting from the integration are shown in Fig. 4. The three cases of heating parameters reported in Sect. 3 have been chosen to put in evidence some properties of these solutions. In fact, three important considerations can be derived from the comparison of the profiles:

I) the maximum attained temperature is just above the temperature of the second crossing between H and L functions and therefore it is higher for *Cases 1a* and $1c$;

II) when the maximum attained temperature is larger than $10^6\ K$ the cold cloud core has a negligible extension ($x < 10^4$) in comparison with the hot external shell of the cloud ($x \simeq 10^8$).

III) the temperature profile does not depend on the heating function except in the cloud core (compare *Cases 1a* and *1c*).

The three above points can be easily understood on the basis of the energy equation. For the first one the energy equation must be multiplied by $[r^2T^{5/2}\frac{\partial T}{\partial r}]$ and then integrated to give

$$\frac{\kappa_o}{2}\left[[r^2T^{5/2}\frac{\partial T}{\partial r}]^2\right]_{T_o}^{T_M} = 0 =$$

$$= \int_{T_o}^{T_M} r^4[L(p,T) - H(p,T)]T^{5/2}dT.$$

This expression implies that regions with positive and negative values of $(L-H)$ weighted by $(r^4T^{5/2})$ must compensate in the cloud but also shows that the weight of the hotter external cloud region with $(L-H) < 0$ is enhanced by the increased value of the term $(r^4T^{2/5})$. For this reason the integral vanishes, and hence $\frac{\partial T}{\partial r} = 0$, just after the crossing.

To explain the second point, it is useful to derive from Eq. (3) a value for the typical length scale, X, of the temperature variation at the temperature minimum and maximum (where $dT/dr = 0$):

$$X \simeq \left[\frac{1}{T}\frac{\partial^2 T}{\partial r^2}\right]^{-\frac{1}{2}} \simeq \left[\frac{L-H}{\kappa_o T^{7/2}}\right]^{-\frac{1}{2}}. \qquad (9)$$

From the above expression it can be easily understood why the the cold and the hot phases in the same cloud can show so different length scales. In fact, for low temperatures $(L-H)$ has a maximum thus contributing to make X smaller than it is at high temperatures. Actually, a loss function increasing with temperature ($L \propto T^{7/2}$) would be necessary to have a comparable extension of the cold and hot part in the same cloud while for a thin plasma the opposite holds since it is $L \propto n^2T^q \propto p^2T^{q-2}$ with $q < 0.5$ for $T > 10^5$.

Another possibility to obtain a wide cold central region seems that of starting from a value of T_o where L and H balance each other "exactly" as in the case of no conduction (see Sect. 2.2). To test this possibility in *Cases 1a* and $1b$ the heating constant has been chosen so as $H(p,T_o) = L(p,T_o)(1-\epsilon)$ with $\epsilon << 1$. Very low values of ϵ, down to $5\ 10^{-6}$ have been tested in order to reproduce the cold equilibrium phase but no appreciable change is observable in the results for ϵ smaller than $1\ 10^{-3}$. This numerical result does not seem compatible with expression (9) for the typical length scale and with the intuitive idea that a continuous variety of temperature profiles (ranging from a very steep one to a constant one) must exist. However, these numerical results can be analytically confirmed. In fact, a Taylor expansion of the temperature around $r = 0$ shows that the temperature is almost constant, i.e. the solution $T(r) \simeq T_0$ holds, only for $r < r_*$ where r_* is the convergence radius of the series. As Appendix B shows this radius does not scale as ϵ^{-1}, i.e. does not imply a larger and larger constant temperature region as ϵ goes to zero. So, in the range of applicability of the Taylor expansion ($r < r_*$) even if ϵ is very small, the flat central region is very narrow and the cloud is globally a hot one. When $\epsilon << 1$ ($L \simeq H$) the only difference with respect to the case in which $L(p,T_o) > H(p,T_o)$ (*Case 1c*) is that the narrow cold region in the cloud center has a flatter temperature profile.

For point III) it is apparent that for most of the cloud extension the relationship $L > H$ holds, hence the heating function does not influence the temperature profile except just in the center, as explained in point II. In fact, at high temperature where $L = H$ the relative weight of both loss and heating with respect to the first and the second derivatives of the temperature arising from the left hand side of Eq. (3) is small. Therefore, the temperature profile results almost the same even if the slope of the heating function is very different (compare *Cases 1a* and $1c$).

This part of the analysis leads to the conclusion that it is the value of the temperature at which heating and loss functions cross each other which determines the overall features of the temperature profile. The form of the heating function is important only because determines this value while the heating intensity and its temperature dependence have no appreciable influence on the temperature profile.

4.2. The influence of different loss functions

Having analyzed the influence of different heating functions we now analyze the influence of different loss functions on the temperature profiles. We remember that, as explained in Sect. 3, the reduced loss function is a sign of a different energy balance in the plasma between matter and radiation. In particular the expression (8) used for *Case 2a* includes photo-ionization heating and Compton cooling.

The same integration as above has been carried on for the other two cases of loss and heating functions with Ξ ranging from 0.1 to 10. As an example, in Fig. 5 the temperature profiles computed for *Cases 1a* and for *Cases 2a* and *3a* with $\Xi = 1$ are compared. The temperature profiles correspond to loss and heating functions shown in Figs. 1,2 and 3. The general features are as described in Sect. 4.1 for *Case 1*. In fact, even if a wider central cold region develops for decreasing losses, i.e. going from *Case 1* to *Case 3*, the cold region ($T < 10^6 K$) still occupies less than one thousandth of the cloud radius. The trend observed going from *Cases 1a* to *3a* confirms the deduction of the previous subsection about the importance of the loss function slope.

The results of this section show how the idea that conduction only smooths steep gradients is misleading. In fact, in a stationary and static configuration the extension of the cold region is determined by the introduction of thermal conduction and results very narrow. This fact has serious consequences for the cloud emission, as explained below, and cannot easily be changed. Neither a different mechanical heating nor the pres-

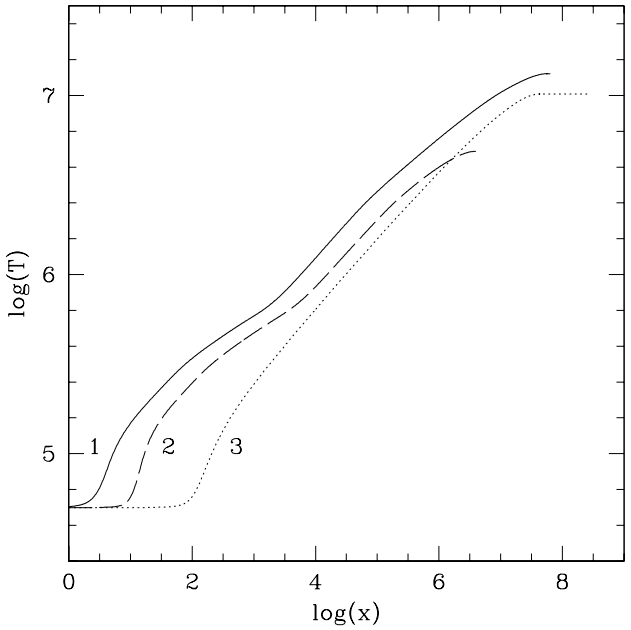

Fig. 5. Cloud temperature profiles for the three cases $1a$, $2a$ and $3a$ relative to the loss functions shown in Figs. 1,2 and 3.

ence of a radiative heating or of a different loss function can produce a large cold cloud.

5. The cloud emission

In order to compute the cloud luminosity it is necessary to know its opacity. For the cloud configurations derived in the preceding sections the optical depth at $\nu = 10^{15} Hz$, τ_{15}, and the scattering depth , τ_s, can be written as

$$\tau_{15} = 2.4\ 10^{-36} \frac{n_o^2 Z}{T_o^{1/2}} \int_0^{x_M} g(T)(1 - e^{\frac{-4.8\ 10^4}{T}})(\frac{n}{n_o})^2 \frac{dx}{\theta^{1/2}} \simeq$$

$$\simeq 6\ 10^{-24} n_o T_o^{1/4} \int_0^{x_M} g(T)(\frac{n}{n_o})^2 \frac{dx}{\theta^{3/2}}$$

$$\tau_s = 6.6\ 10^{-25} n_o Z \int_{-x_M}^{x_M} (\frac{n}{n_o}) dx \simeq$$

$$\simeq 1.3\ 10^{-16} T_o^{7/4} \int_0^{x_M} (\frac{n}{n_o}) dx.$$

where relationships (4) and (5) have been taken into account. In these expressions all the parameter dependence is explicit and the integrals provide only numerical factors.

Owing to the fact that cloud dimensions scale with the inverse of density (Eq. (5)), τ_s does not depend on the cloud density, hence its value is fixed for each model. For every tested configuration τ_s was always much less than one thus implying that in this framework optically thin cloud thick to scattering cannot exist.

For the optical depth, τ_{15}, the situation is different and it can become larger than unity for increasing density. For the temperature profiles shown in Sect. 4 for the case of coronal radiative losses, we obtain $\tau_{15} \simeq 2\ 10^{-20} n_o$ for the three cases since it is the cold core which mainly contributes to the opacity. Hence, very high density values are necessary to make the cloud thick.

Since the condensations analyzed here are thin their thermal emission can be easily computed from the standard free-free expression

$$\epsilon_\nu(r) = 9.4\ 10^{-37} \int_0^r g(\nu, T) \frac{n^2}{T^{1/2}} r^2 dr \quad \frac{erg}{Hz\ sec} \qquad (10)$$

where $g(\nu, T)$ is the Gaunt factor which takes into account free-free, free-bound and two photons contributions. For the Gaunt factor we use here the approximation introduced by Mewe et al. (1985) computed for $\nu \simeq 10^{15} Hz$

$$g(10^{15}, T) = 27.83(10^{-6}T + 0.65)^{-1.33} + 2.28(10^{-6}T)^{0.422}$$

for $T \geq 2\ 10^5 K$ and we assume $g(T) = g(2\ 10^5)$ for $T < 2\ 10^5 K$.

Computing the above expression for $\nu = 10^{15} Hz$, writing the density in terms of the central density n_o and pressure p_o

$$n = n_o \frac{p(x)}{p_o} \frac{T_o}{T(x)} = \frac{n_o}{\theta} \frac{p}{p_o}$$

and substituting the dimensionless quantities defined above, the cloud luminosity results

$$L_{cloud}(R) = 3.\ 10^{18}\ \frac{n_o T_o^{5/4}}{x_M^2}$$

$$\times \int_0^{x_M} g(T) \left(\frac{p}{p_o}\right)^2 \theta^{-5/2} x^2 dx \quad \frac{erg}{sec}. \qquad (11)$$

Each shell of the cloud contributes to the global luminosity with the amount

$$\Delta L_{cloud}(x) = 3.\ 10^{18}\ \frac{n_o T_o^{5/4}}{x_M^2} \int_x^{x+\Delta x} g(\theta)(\frac{p}{p_o})^2 \theta^{-5/2} x^2 dx$$

$$\propto \left(\frac{p}{p_o}\right)^2 x^2 \theta^{-2.5} \Delta x. \qquad (12)$$

The ΔL_{cloud} profile for the *Case 1a* is shown in Fig. 6. It is apparent that this quantity increases with the radius, hence, as one can deduce for Eq. (12), the temperature ($\equiv \theta$) growth does not arrive to compensate the increasing emitting volume. The pressure term does not help since, for the moment, pressure is held constant and hence $p/p_0 = 1$. Therefore, the emission contribution from the cold and dense core (with a high specific emission) is negligible compared to the emission of the extended outer part of the cloud and of the confining medium. Hence, these clouds will never show a thermal spectrum characterized by a temperature ranging from 10^5 to 10^6 K. Changing the functions and parameters entering the energy equation does not change the results of this section. Hence these constant pressure

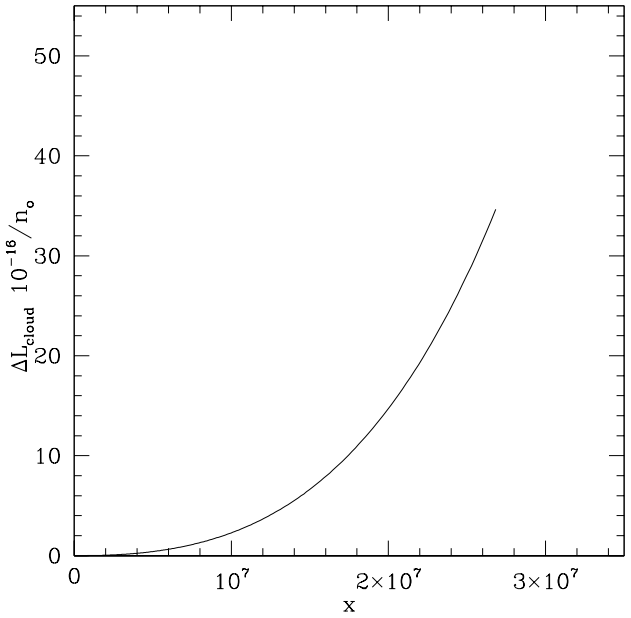

Fig. 6. Differential luminosity for the case of coronal losses and of heating function a

stationary clouds cannot be an explanation for the UV emission in AGN.

Before stating that cold condensations cannot be invoked at all for explaining UV emission in AGN it is necessary to analyze if the modification of some of the initial hypothesis can change the picture.

6. The role of pressure gradients

The results of Sects. 4 and 5 have been derived in the hypothesis that the whole cloud as well as the confining medium have the same pressure. Generally this is not the case since some forces, at least gravity, will in reality act on the system. The influence of the cloud self-gravitation can be estimated computing, for each derived temperature profile the related pressure gradients. Integrating the hydrostatic equation

$$\frac{\partial p}{\partial r} = -m_H n(r) \frac{4\pi G}{r^2} \int_0^r m_H n\, r_1^2 dr_1$$

the pressure profile can be easily computed.

For all the analyzed models the assumed constant pressure profile is not altered by the introduction of gravity. Only for low central densities the pressure profile can change somewhat because clouds in this limit become very large (see Eq. (5)) and their external layers feel the presence of inside matter, for example $p(R)/p_o = 0.997$ for $n_o = 10^{10}\ cm^{-3}$.

In order to weigh the influence of different force profiles on the results of the preceding section, since it is not possible to examine all the unknown forces which may act on our system, we have adopted an externally imposed pressure profile. This pressure profile, whose shape we can arbitrarily modify, has been substituted to the flat pressure profile in the energy equation. We have then calculated the temperature and luminosity for steeper and steeper pressure profiles. It results that the temperature is not very sensitive to a pressure gradient: only the hot almost constant temperature part of the cloud may become more extended. Luminosity, on the contrary, is more affected, since, as Eq. (12) shows, decreasing the pressure in the external layers causes a decrease of the emission from these layers. This is clearly visible in Fig. 7 where ΔL_{cloud} is shown, for three different values of the ratio of the external to the central pressure, for the pressure profile $p(x) = p_o\, e^{-(x/\sigma)^2}$.

As it appears from Fig. 7, introducing pressure gradients inside the condensation makes it possible to obtain bright clouds. To be sure about that, the emission from the external confining medium should be estimated and compared to the global cloud emission. However, from Fig. 7 it is apparent that to shift the peak of the emission towards the cloud center very strong pressure gradients are necessary. For example, a ratio of the external to the central pressure $p_{ext}/p_o = 1.7\,10^{-5}$ is necessary to place the luminosity maximum around one fourth of the cloud radius, i.e. around $x \simeq 6\ 10^6$. At this distance from the cloud center the temperature is not too far from $10^7 K$, as it appears from the temperature profile shown in Fig. 4 for the same *Case 1a*. Hence, even in this case, the temperature corresponding to the peak of luminosity is almost equal to the external temperature value: a thermal peak with $T \sim 10^5 - 10^6 K$ cannot be observed in the spectra emitted from such a cloud. As a matter of fact, in any tried realistic case the luminosity does not peak in the central part of the cloud, corresponding to the cold core, but peaks in its external part which has almost the same temperature of the external medium. Hence, even if the cloud now is more luminous than the surrounding medium, the real emitting region cannot be observed as a region of cool plasma but only as a region of enhanced density at the same temperature as all other plasma.

We conclude that self gravitation does not have any influence on the equilibrium of dense clouds and that the introduction of high pressure gradients inside the cloud is necessary to make the external hot part of clouds brighter than their surroundings but does not substantially modify the temperature structure and hence does not make the cold core more visible.

7. Magnetic field importance

The influence of the presence of a magnetic field, **B**, in the above configuration is of two different kinds.

First it can act by adding to the momentum equation the contributions of magnetic tension and pressure, thus changing the pressure equilibrium profile inside the cloud. As it has been analyzed in Sect. 6 a strong pressure gradient is necessary to have bright clouds and magnetic field could help to establish this gradient. However, the magnetic field can compress the plasma only perpendicularly to its line of force thus the most natural geometry for the condensation is a filament aligned to the field. Celotti et al. (1992) have suggested the presence of such condensations in the central regions of AGNs.

Second, the magnetic field acts as a constraint for the heat conduction. In fact, the ratio between conduction parallel and

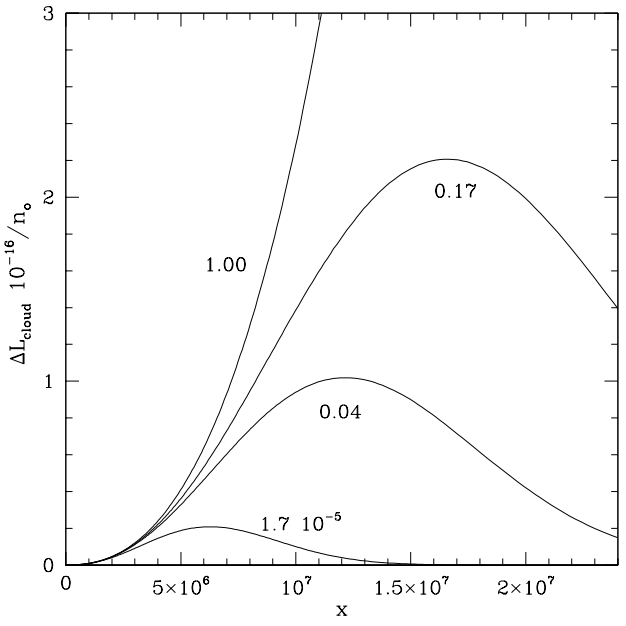

Fig. 7. Differential luminosity for the case of coronal losses and heating function a and different pressure gradients inside the cloud. The curves are labeled with the ratio of the external to central pressure p_{ext}/p_o. The curve labeled with 1.00 is therefore the same of Fig. 6.

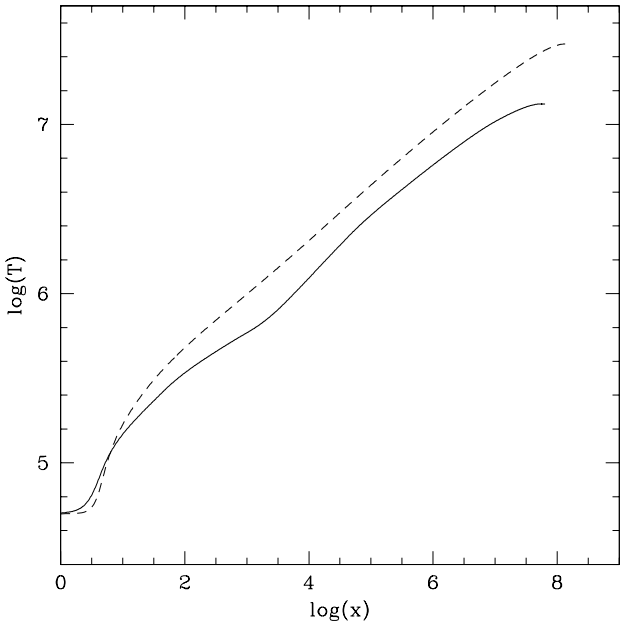

Fig. 8. Cloud temperature profile for coronal radiative losses and for heating function a with (dashed line) and without (continuous line) the magnetic field, i.e. in a planar and in a spherical geometry, respectively.

perpendicular to magnetic lines of force is generally much bigger than one, thus implying that heat is mainly transported along magnetic field lines. In our case the existence of a preferential direction for heat conduction changes the geometry of the system from spherical to planar. In fact, the heat transport and balance must be computed only along magnetic field lines of force while along planes perpendicular to magnetic field lines different temperature values can freely coexist if $L = H$ is satisfied.

In general we can say that the picture can be very different from that envisaged in the previous sections, since, instead of having blobs entrained in the flow of their confining medium, it is now possible to have condensations in form of filaments following the magnetic field geometry and anchored by magnetic field tension against other external forces (gravity, for example). The specific configuration is clearly determined by the structure of the magnetic field itself.

To perform the same analysis developed before for the spherical geometry in this new configuration we have to solve the energy equation along a coordinate parallel to **B**, i.e. in planar geometry. With the same approximations used above, the energy equation reads

$$\kappa_o \frac{\partial}{\partial s}[T^{5/2}\frac{\partial T}{\partial s}] = L(p,T) - H(p,T)$$

where s is the coordinate along the magnetic field line. As before the pressure profile is given from outside and, since it is its profile along the magnetic line of force which enters the above equation, it may be held constant or can vary independently of the presence of **B**. Nothing is specified in the direction perpendicular to the magnetic field and in this sense our analysis is complementary to that of Kuncic et al. (1996, 1997) who derive the condensation structure without conduction, i.e. in the direction perpendicular to **B**.

In Fig. 8 we report, for comparison, the temperature profile for the *Case 1a* with and without magnetic field. The change of the geometry makes the condensation more extended and the maximum temperature higher but does not substantially change the results obtained in the previous sections. Hence, all the problems related to the distribution of its emission are still present even if the extension of this sheet can be freely chosen (in any case $< R_{UV}^2$). Actually there is not a big difference between a continuous slab and a sequence of small clouds from the point of view of their emission.

It is important to note that the above conclusions have been derived taking into account the presence of the magnetic field, however they can be extended to any situation in which a planar geometry is a better description than a spherical one. From the comparison between the results in spherical and in planar geometry it follows that in this case the assumed geometry has no consequences for the reproducibility of UV emission from AGN in terms of thin cold condensations.

The above considerations deal with ordered magnetic fields and do not consider tangled fields. The presence of random magnetic field fluctuations has been proposed to suppress thermal conduction in different astrophysical contexts (cooling flows, for example). One can suppose that the coherence length of the field, if smaller than the particle mean free path, can assume the role of the particle mean free path thus suppressing thermal conduction. The reason why this possibility has not been taken into account here lies in the fact that we are interested in a non turbulent plasma, while plasma conduction is suppressed only if

the fluctuating magnetic field is dynamically important (Rosner & Tucker 1989). In addition, a recent analysis shows that it does not seem possible to stretch magnetic field lines sufficiently to suppress thermal conduction (Tao 1995).

8. Testing the model self-consistency

In the preceding sections we have assumed that the emitting clouds have already attained an equilibrium configuration since both in the momentum and in the energy equation the partial derivative with respect to time as well as the terms taking into account plasma flow have been disregarded.

Unbalanced forces induce in the plasma matter deplacements through which the plasma tries to find , if possible, a new equilibrium configuration. The typical time related to this dynamical evolution is the sound crossing time, t_{sound}, which order of magnitude is

$$t_{sound} \simeq \frac{r}{c_{sound}} \simeq 10^{-4}\frac{r}{T^{1/2}}. \quad sec$$

It is evident (see Figs. 4 and 5) that the extension of the central cold part of the cloud (i.e. where $T \leq 10^6 K$) is limited by $x < 10^4$. Hence, using Eq. (4) and the expression for Z previously derived, the sound crossing time for the cold core is $t_{sound} < 10^{13}/n_o\ sec$. For the density values necessary to reproduce the observed UV emission in the limit $\tau_{15} < 1, \tau_s < 1$, i.e. for $n_o > 10^{12} cm^{-3}$ (Barvainis 1993) these times are very short. This fact implies that if the clouds are not in pressure equilibrium, or cannot evolve into such a configuration, they will rapidly dissolve.

Almost the same argument supports the assumption of a stationary configuration. In fact, the time evolution of the cloud temperature is controlled by the omitted term in Eq. (3)

$$\frac{\rho^\gamma}{\gamma - 1}\frac{\partial(p\rho^{-\gamma})}{\partial t}$$

from which an order of magnitude of the radiative time, t_{rad}, can be derived as

$$t_{rad} \simeq \frac{p}{\mid L - H \mid}. \quad sec$$

Exactly computed for all analyzed configurations, this time also turns out to be very short ($\simeq 25\ t_{sound}$) thus implying a very fast evolution for the cloud if Eq. (3) is not exactly verified.

All the above considerations confirm that the model developed in the previous sections is self-consistent.

9. Evolving configurations

In the previous sections we have analyzed the possible equilibrium configurations of a cold cloud, however, a different scenario can be also envisaged. Suppose that somehow big cold blobs of plasma form or are injected in the hot medium. These blobs of radius r_o will find themselves in a non-equilibrium situation and will then evolve, if possible, towards one of the configurations derived in the previous sections. The cases of uniform constant temperature clouds investigated by many authors (and outlined in Sect. 2.2) may correspond to this scenario in which heating and losses balance each other both at T_o and T_{hot}, the temperature of the cold cloud and of the hot external medium, respectively. This ideal situation is influenced by the presence of thermal conduction which smooths the boundary between the hot and cold plasma giving rise to a region of intermediate temperature like that shown in Fig. 4, for example. However, the temperature profile

$$T(r \leq r_o) = T_o$$
$$T(r_o \leq r \leq r_M) = T(r)$$
$$T(r \geq r_M) = T_{hot}$$

is not the solution of the static and stationary energy equation, hence this type of cloud configuration changes in time. Since the cloud emission is proportional to the cloud volume, also the emission of these evolving clouds changes in time. If r_o is the radius of the constant temperature core, when r_o decreases of a factor of two the emission is reduced of 1/8 thus implying that a new cloud must be already present to keep the emission at an almost constant value. For this kind of non-equilibrium configurations the typical time-scale of cloud evolution is the sound crossing time. Hence the time interval during which the cloud emission is reduced of 1/8 is t_{sound} computed for $r = r_o/2$, i.e.

$$t_* = t_{sound}(r_o/2) = 5\ 10^{-5} r_o T^{-1/2} \quad sec$$

The value of the core radius r_o can be written in terms of other physical quantities as Barvainis (1993) does:

$$r_o = 8.1\ 10^8 \frac{\tau_s^2}{\tau_{15}} T_5^{-1.3} \quad cm$$

where τ_s, τ_{15} and $T_5 = T_o/10^5$ are the scattering and the optical depth and the temperature of the central uniform region, respectively.

If one deals with sources thin to scatter or with small high density clouds (Barvainis's case 2, Celotti et al. 1992) the reduced dimensions assure a rapid evolution: $r_o < 5\ 10^{10} cm$ implies $t_* < 1\ hour$. The life-time of these evolving clouds is hence very short.

It can be easily shown (see Appendix C) that the condition $r_o < 5\ 10^{10} cm$ holds for most thin sources i.e. for sources which have a small total effective optical depth,τ_{tot}:

$$\tau_{tot} = \sqrt{\tau_{15}(\tau_{15} + \tau_s)} < 1.$$

In conclusion, for most sources (all those thin to scatter, most of those with total effective depth less than one and those with $\tau_s > 1$ and $\tau_{tot} > 1$, but with reduced dimensions) the evolution is very rapid. A model in which the UV emission is due to evolving clouds whose birth is not clear (nobody has solved this point) and which disappear in less than one hour does not seem very realistic.

The same conclusion is not true for large clouds having $\tau_s > 1$ and $\tau_{tot} > 1$ (Collin-Souffrin S. et al., 1996) and/or in a different framework (BLR, for examples). In such cases clouds can evolve on longer time-scales thus not requiring a high rate of clouds production.

10. Conclusions

In this paper the equilibrium structure of a cold configuration embedded in a hot plasma has been investigated. The energy equation has been numerically solved consistently with momentum equation and the temperature profile inside the cloud has been derived. From these computations we derive that cloud self gravitation can be safely ignored while thermal conduction must be taken into account since the pictures resulting from the energy equation with or without thermal conduction are very different. In particular the introduction of the conducting term provides a defined length for the cloud extension which otherwise is undetermined. The importance of this point is that it strongly affects the computation of the UV emission from the cloud. In fact, the temperature profile inside the condensation, as it results from the integration of the energy equation, shows only a very narrow cold region. Starting from the cold cloud core the plasma temperature rises very sharply and then smoothly, in a wide region, joints the external temperature. Hence the largest part of the cloud is at a temperature which is only slightly less than that of the external medium. Since the cold region extension is negligible in comparison with that of the hotter external part of the cloud, its emission too is very low.

A variety of heating functions have been tested with no difference in the conclusions apart from the value of the temperature of the external medium which results determined by the intersection of heating and losses. Radiative losses have also been changed, always in the optically thin approximation framework, ranging from the pure coronal case to a case of reduced losses (at low temperature) which can represent the effect of photoionization. The fact that most results are not very sensitive to the chosen loss and heating functions can be easily understood as due to the intrinsic nature of all tried radiative losses, i.e. to the fact that in a thin plasma radiative losses have their maximum at low temperatures, essentially owing to the n^2 dependence (see Sect. 4 for details). In conclusion, the relative extension of the cold and warm regions does not depend on the type of heating and on the presence of external radiation, only the existence of a loss function increasing with the temperature ($L \propto T^{7/2}$) could change it.

In addition to the main points discussed above other important conclusions can be derived from our analysis:

1)To obtain a cloud radiating more than the external medium it is necessary to make the cloud over-pressured in comparison to the external medium. Apart from the problem of how these strong pressure gradients could be produced, even in this case the emission peaks in the external warmer part of the cloud and not in its central cold part. In the hypothesis that the external medium is hotter than $10^5 - 10^6\ K$ these condensations cannot reproduce the observed UV and soft-X ray spectra.

2)Clouds are thin to scattering independently of the the cloud density since cloud dimensions scale inversely with the density itself. Hence stationary and static cold clouds optically thin to radiation but thick to scattering do not exist.

3)The introduction of magnetic field makes the geometry change from spherical to planar since conduction has a preferential direction along the magnetic lines of force. However, this fact does not change all the conclusions listed above.

4)Non-equilibrium configurations with large cold cores suitable to reproduce the observed emission generally have a very rapid evolution. A model based on such configurations is therefore not very realistic.

Taking into account also Kuncic et al.(1997) results which, covering a higher range of densities, are complementary to the ones presented here, we can conclude that the possibility of explaining the AGN blue bump by thermal *thin* emission from cold condensed matter does not seem very realistic.

Acknowledgements. We wish to thank Prof. L.Woltjer, Prof. C.Chiuderi and Prof. M.Salvati for their critical reading the original version of the paper and for some helpful comments.

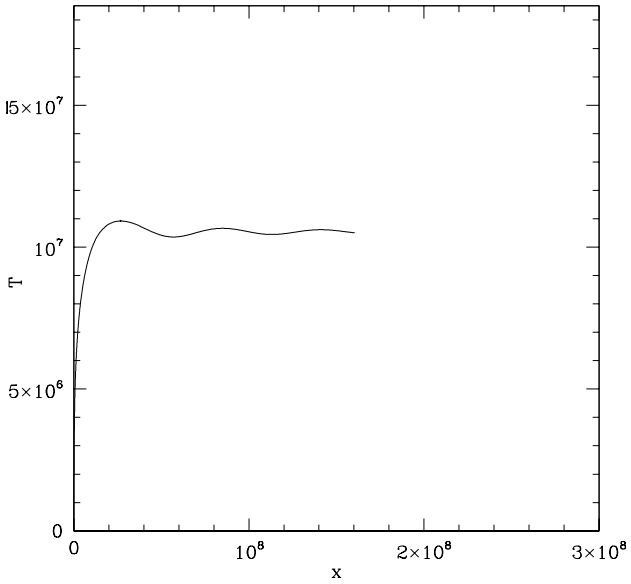

Fig. A1. Temperature profiles for *Case 1a* for the cloud and for a part of the external medium around the cloud. The peak in the temperature identifies the boundary between the cloud and the external medium.

Appendix A: a different boundary for the cold cloud

At the cloud boundary a rather high negative value of d^2T/dx^2 is found, for every heating function we tried. To investigate whether a better connection between the external medium and the cloud is possible the integration has been carried out for larger radii.

The result is shown in Fig. A1 for *Case 1a*, but is analogous in all other cases. Between the cloud, i.e. the region where $T < T_M$ (T_M being the maximum attained temperature) and the uniform confining medium there is an intermediate region wide about ten times the cloud radius, where the temperature oscillates around a specific value T_*. This temperature value is exactly that of the intersection between heating and loss functions. Also if a third intersection between heating and losses exists at higher temperature the asymptotic temperature is determined by the intersection corresponding to the change from $(L - H) > 0$ to $(L - H) < 0$ for increasing temperature.

In fact, around this intersection only the temperature value can oscillate between relative minima with positive second derivatives and relative maxima with negative $d^2T/dx^2 \propto L-H$ (see Eq. (3)). As a consequence, the confining medium, must have a temperature for which $\frac{\partial[(L-H)/n]}{\partial T}|_{p=const.} < 0$, and is unstable. This fact constitutes another substantial difference between the case with and without conduction and shows how useless is the search of stable intersections of loss and heating functions at higher temperatures in a spherical geometry.

Appendix B: analytical approximation for the temperature profile in the cloud core

The temperature profile around $r = 0$ can be obtained as a Taylor expansion

$$T(r) = T(0) + \sum_{n=1}^{\infty} \left(\frac{\partial^n T}{\partial r^n}\right) \frac{r^n}{n!}.$$

All the coefficients, except the two defined by the boundary conditions shown in Sect. 2.3, can be determined by deriving Eq. (3) with respect to r and by computing the second and all the successive derivatives in the limit $r \to 0$ (making use of the Hopital rule). In this way the Taylor expansion becomes:

$$T(r) = T(0) + \frac{r^2}{6\kappa_o} T_o^{-5/2} Y_o + \frac{r^4}{120\kappa_o^2} T_o^{-6} Y_o \left[T_o \Delta Y_o - \frac{25}{6} Y_o\right] + ... \quad \text{(B1)}$$

where

$$Y_o = [L(p, T_o) - H(p, T_o)]$$

and

$$\Delta Y_o = \left[\frac{\partial[L(p,T) - H(p,T)]}{\partial T}\right]_{r=0}.$$

Then, using the position $H(p, T_o) = L(p, T_o)(1-\epsilon) = L_o(1-\epsilon)$, Eq. (B1) becomes

$$T(r) = T_o + \frac{r^2}{6\kappa_o} T_o^{-5/2} L_o \epsilon + \frac{r^4}{120\kappa_o^2} T_o^{-6} L_o \epsilon \left(T_o \Delta Y_o - \frac{25}{6} L_o \epsilon\right) + ... \quad \text{(B2)}$$

In the limit of small ϵ, in which we are interested,

$$T_o \Delta Y_o = T_o \left[\frac{\partial[L(p,T) - H(p,T)]}{\partial T}\right]_o >> \frac{25}{6} L_o \epsilon$$

since the function L and H do not have the same derivative in $T = T_o$. For *Case 1a*, for example,

$$T_o \Delta Y_o = 3L_o + 2.25\ H_o = [5.25 - 2.25\epsilon]\ L_o$$

which does not vanish for vanishing ϵ. Hence, for small ϵs the Taylor expansion can be approximated as:

$$T(r) = T_o + \frac{r^2}{6\kappa_o} T_o^{-5/2} L_o \epsilon \left[1 + \frac{r^2}{20\kappa_o} T_o^{-5/2} \Delta Y_o + ...\right].$$

This expression is a good solution of Eq. (3) for $r < r_*$ where r_* is the convergence radius of the series in the square bracket. It is out of the purpose of the present analysis to determine r_*; what it is important is to realize that r_*^2 does not scale as ϵ^{-1}, as the second term in the square bracket shows. Hence, decreasing ϵ does not imply an increase of r_*. What happens for vanishing ϵ is that the term added to the constant central temperature also vanishes, but only if the series does not diverge. Hence, the temperature profile becomes flatter and flatter in the interval of convergence of the series while the amplitude of the interval itself does not have an evident dependence on ϵ.

Appendix C: the relationship between cloud extension and luminosity

This Appendix shows that the condition $r_o < 5\ 10^{10} cm$ holds for most sources if these sources have a small total effective optical depth,τ_{tot}:

$$\tau_{tot} = \sqrt{\tau_{15}(\tau_{15} + \tau_s)} < 1.$$

To understand this point the quantities τ_s and τ_{15} must be derived from the expression for the luminosity (Barvainis 1993)

$$L_{46} \simeq 9.7\ R_{16}^2 f T_5 \tau_{15} \qquad erg\ sec^{-1}$$

and the condition

$$\tau_{tot} \simeq \sqrt{\tau_{15}\tau_s}$$

derived from the above expression for τ_{tot} in the limit $\tau_s > \tau_{15}$. Here L_{46} is the luminosity in units of 10^{46}, computed for $\nu = 10^{15} Hz$, R_{16} is the dimension of the overall emitting region in units of 10^{16} ($R \leq R_{UV}$) and f is the covering factor which the presence of the large conductive shell around each cloud makes less than one.

Substituting the expressions for τ_s and τ_{15} in that for r_o one obtains

$$r_o = 9.2\ 10^6 R_{16}^6 T_5^{1.7} L_{46}^{-3}\ \ cm$$

where $f = 0.5$ and $\tau_{tot} = 0.1$ have been assumed. For low luminosity sources one can fix $T_5 = 1$ and $R_{16} \lesssim 0.3$ and derive

$$r_o \lesssim 6.7\ 10^3 L_{46}^{-3}\ \ cm$$

from which one can easily infer $r_o > 5\ 10^{10}\ cm$ for $L_{46} < 5\ 10^{-3}\ erg/sec$. Hence, only low luminosity Seyfert can be modeled with clouds evolving on time-scales longer than one hour.

References

Barvainis R., 1993, ApJ 412, 513
Celotti A. & Fabian A.C. Rees M.J., 1992, MNRAS 255, 419
Clavel J. et al., 1991, ApJ 366, 64
Collin-Souffrin S., 1991, Proc. Colloq. 'Testing the AGN paradigm', University of Maryland October 14-16, p.119
Collin-Souffrin S. et al., 1996, A&A 314, 393
Courvoisier T. J.-L. & Clavel J., 1991, A&A 248, 389
Field G. B., 1965, ApJ 142, 531
Fiore et al., 1995, ApJ 449, 74

Gehrels N. & Williams E.D., 1993, ApJ 418, L25
Gonçalves D.R., Jatenco-Pereira V., Opher R., 1993, ApJ 414, 57
Gonçalves D.R., Jatenco-Pereira V., Opher R., 1996, ApJ 463, 489
Haardt F., Maraschi L., Ghisellini G., 1994, ApJ 432, L95
Krolik J.H., McKee C.F., Tarter C.B., 1981, ApJ 249, 422
Kuncic Z., Blackman E.G., Rees M.J., 1996, MNRAS 283, 1322
Kuncic Z., Celotti A., Rees M.J., 1997, MNRAS 284, 717
Lightman A.P. & White T. R., 1988, ApJ 335, 57
Mathews W. G. & Doane J. S., 1990, ApJ 352, 42
Mewe R., 1990, In: Physical processes in hot cosmic plasmas, W.Brinkmann et al. (eds.) , Kluwer Academic Publ., The Netherlands, p.39
Mewe R. , Lemen J.R., van den Oord G. H. J., 1985, A&AS 62, 197
Raymond J.C. & Smith B. W., 1977, ApJS 35, 419
Reynolds C.S. & Fabian A.C., 1995, MNRAS 273, 116
Rosner R., Tucker W. H. , 1989, ApJ 338, 761
Rosner R., Tucker W. H. , Vaiana G. S. , 1978, ApJ 220, 643
Ross R. R., Fabian A.C., Mineshige S., 1992, MNRAS 258, 189
Shields G.A., 1978, Nature 272, 706
Siemiginowska A. et al., 1995, ApJ 454, 77
Sivron R. & Tsuruta S., 1993, ApJ 402, 420
Spitzer L., 1962, In: Physics of fully Ionized Gases, Interscience, New York
Tao L., 1995, MNRAS 275, 965
Walter R. & Fink H.H., 1993, A&A 274, 105
Wilson R. , 1962, J.Quant.Spectr.Radiat.Transfer 2, 477
Zdziarski A. A. et al., 1995, ApJ 438, L63
Życki P.T., Collin-Souffrin S., Czerny B., 1995, MNRAS 277, 70